Proceedings of the 17th International Symposium on the Packaging and Transportation of Radioactive Materials
PATRAM 2013
August 18-23, 2013, San Francisco, CA, USA

APPLICATION FOR TRANSPORTATION CASK GEOMETRY WITH MONTE CARLO CODE PHITS TO SHIELDING ANALYSIS

Shinji Goko
JNES

Jiro Katayama
JNES

Japan Nuclear Energy Safety Organization (JNES), Tokyo, Japan

ABSTRACT

For cross-check analysis in JNES, we are examining for applying three-dimensional continuous energy Monte Carlo code PHITS[1] (Particle and Heavy Ion Transport code System) to shielding safety analysis of fuel cask. In this work, PHITS was tested by simulations and their evaluations for some hypothetical damaged transportation cask geometries. Analytical results of PHITS clearly show the specific behavior of each radiation with some kinds of evaluated values and graphical spatial distributions. Accordingly, we expect that PHITS will be effective to evaluate and understand unexpected results.

In future, applying PHITS to shielding safety analysis of fuel casks will become powerful tool by optimizing calculation method, benchmark analysis and so on.

INTRODUCTION

In Japan, mainly two-dimensional analysis codes, such as DOT[2], have been used in shielding safety analysis for nuclear fuel cask design approval. Such analysis codes are based on the discrete ordinate S_N method. Fuel casks have a basically cylindrical shape; accordingly, their geometry can easily be expressed as a two-dimensional model using a cylindrical system. However, some regions such as fuel assemblies, fuel baskets, and trunnions have complex structures, and thus approximation by approaches such as shape simplification and component homogenization is required to evaluate their shielding analysis. This is also true for simulation of penetration holes, which are expected to be formed in drop tests. Such approximation and analysis codes contain uncertainty factors. Accordingly, to avoid overestimating the shielding safety performance of target fuel casks, shielding safety analysis is generally performed with conservative conditions. MCNP[3], the three-dimensional continuous energy Monte Carlo code, allows us to build an analysis model that can simulate actual design more accurately. For cross-check analysis in JNES, we mainly use MCNP to evaluate both the shielding safety performance of fuel casks and the validity of analysis models used by applicants.

Recently, PHITS, the Particle and Heavy Ion Transport code System, was developed in Japan. PHITS is a three-dimensional continuous energy Monte Carlo code whose performance is equivalent to that of MCNP. This code system has already found applications worldwide in other fields. We are examining the potential of PHITS as a code for analyzing the shielding safety performance of nuclear fuel casks. At first, we analyzed the shielding safety performance of fuel cask geometries assuming various forms of damage as part of a demonstration of the applicability of PHITS to analysis of the shielding safety performance of nuclear fuel casks. This

paper shows the results of analysis of the transportation process of individual radiation in fuel casks and evaluates the influence of damage to casks on the dose equivalent rate.

MONTE CARLO CODE "PHITS"

PHITS is a three-dimensional continuous energy Monte Carlo code; PHITS is based on the nucleon-meson transport code, NMTC/JAM[4] ver. 2, which was developed by the Japan Atomic Energy Research Institute (JAERI, the present Japan Atomic Energy Agency (JAEA)). PHITS was developed through the cooperation of the Research Organization for Information Science and Technology (RIST), Tohoku University, and JAERI/JAEA. Though PHITS has not yet been used to analyze the shielding safety performance of nuclear fuel casks, it has already been used worldwide in a number of fields as will be explained shortly. Thus, the fact that PHITS is a radiation analysis code whose performance is equivalent to that of MCNP has been practically demonstrated in performance analyses of actual equipment and facilities.

Major fields of PHITS application:

- Design and shielding analysis of particle accelerators and neutron sources[5]
- Design of radiotherapy apparatuses and evaluation of exposure due to such apparatuses[6][7]
- Evaluation of radiation environments in exoatmospheric structures[8][9]

Therefore, PHITS can be used as reliable transport simulations in a variety of domains: for example, from an enormous facility to a minute biological cell and from high-energy radiation, such as cosmic rays, to low-energy neutrons for research. PHITS provides various types of tallies to output data, such as track length, current, the heating value, energy deposition, produced nuclides in a geometry, and displacement per atom (DPA). Results obtained from analytical evaluation are not only presented in the forms of numerical values but also are output directly as diagrams, such as graphs and two-dimensional distributions. In addition, some features of PHITS are shown below.

- Geometry : General Geometry (GG) or Combinatorial Geometry (CG)
- Nuclear Data : Ace format (ex. JENDL, ENDF)
- Transportation Particles : Photon, Neutron, Proton, Nucleus, Lepton and so on
- Variance Reduction : Importance, Weight Window, Forced Collisions and so on

ANALYSIS CONDITIONS

For this analysis, we used PHITS version 2.52 and the evaluated nuclear data library JENDL-3.3. Figure 1 shows the geometries of the simulated fuel cask. The simulated fuel cask is cylindrical and consists of a 5.0-cm thick gamma-ray shield (lead) and a 10.0-cm thick neutron shield (resin). A 1.0-cm thick carbon steel structure is attached to each of the following regions: the inside surface of the gamma-ray shield, the outside surface of the neutron shield, and the region between the two shields. Inside the fuel cask, a boron-doped stainless basket grid is installed. In this grid, a total of 16 simulated fuel assemblies are loaded as radiation sources. The space between the basket grid and fuel assemblies is filled with water. The meshes in the regions of lead and resin in Fig. 1 were used for setting the variance reduction parameters (importance).

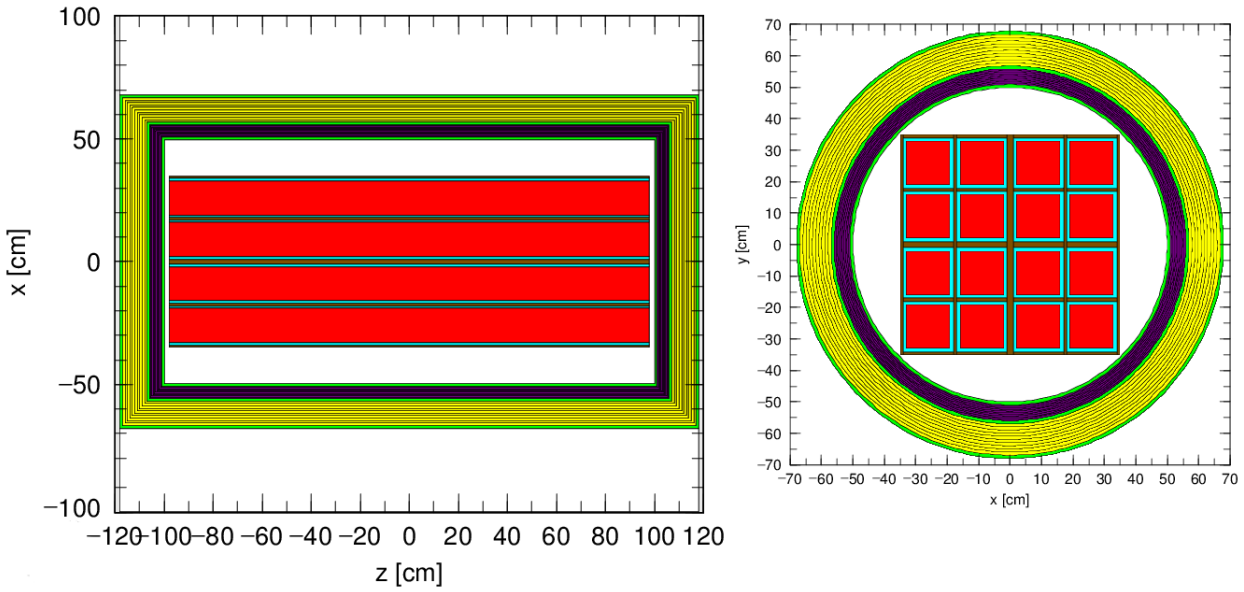

Cross-sectional view for y = 4 [cm] Cross-sectional view for z = 0 [cm]

Fig. 1 Geometry of Simulated Fuel Cask

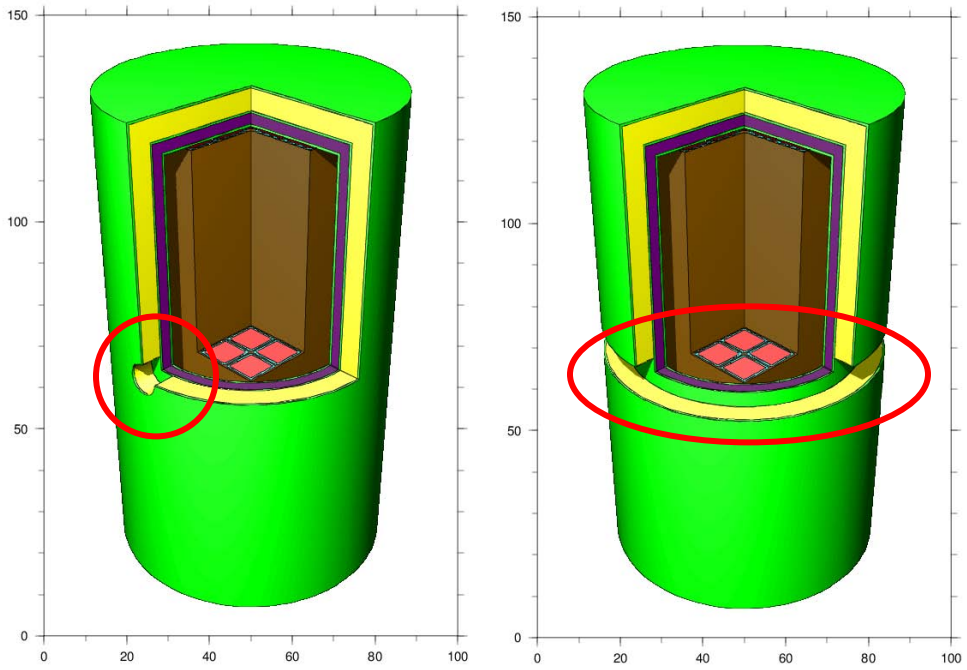

Radial Hole Model (15.0 cm in Diameter) Circumferential Channel Defect Model

Fig. 2 Bird's-eye View of Damage-Simulating Cask Models

Radiation sources :

- Primary gamma-ray spectrum : ORIGEN2 (BWR)
- Neutron spectrum : ^{239}Pu

We expected damage to the fuel cask to form penetration holes leading from the outermost carbon steel region to the resin region of the neutron shield. Accordingly, we simulated for the following seven types of penetration holes formed in the center of the fuel cask in the axial direction (along the z axis). Figure 2 shows bird's-eye views of geometries C) and F) as examples.

A) Radial hole 5.0 cm in diameter
B) Radial hole 10.0 cm in diameter
C) Radial hole 15.0 cm in diameter
D) Tapered Radial hole that widens outward from 5.0 cm to 10.0 cm in diameter
E) Tapered Radial hole that narrows outward from 10.0 cm to 5.0 cm in diameter
F) 15.0-cm wide channel defect formed in the circumferential direction (Circumferential Channel Defect model)
G) 15.0-cm wide channel defect formed in the longitudinal direction (Longitudinal Channel Defect model)

To convert radiation current into their corresponding dose equivalent rates, we used the coefficients[10] of conversion for the one-centimeter dose equivalent rate in accordance with a 1990 recommendation by the International Commission on Radiological Protection.

RESULTS OF ANALYSIS USING THE UNDAMAGED CASK MODEL

Figures 3 and 4 show the results of analysis using the undamaged cask model. Figure 3 shows track length tally outputs that indicates the tracks of each radiation. Figure 4 shows the variations in the current of radiation that have passed through a circle 5.0 cm in diameter on the x axis. Since most of the primary gamma-ray is attenuated in the lead region, only a few of the primary gamma-ray leaks outside. On the other hand, the secondary gamma-ray is generated in outer layer of the lead and the carbon steel region by low energy neutrons which were moderated and back scattered in the resin region; accordingly, a large part of it leaks outside. High-energy neutrons from the radiation sources are relatively monotonously attenuated in the shield. On the contrast, low-energy neutrons near the thermal energy repeatedly increase, decrease, or reflect in each material region. The values and graphs obtained from the analysis using PHITS clearly show the specific behavior of radiation in the fuel cask. In addition, PHITS can also output other types of results, such as the distribution of passing angles at evaluation points and variations in particle transportation over time. Therefore, PHITS allows us to analyze various phenomena occurring in the fuel cask in detail.

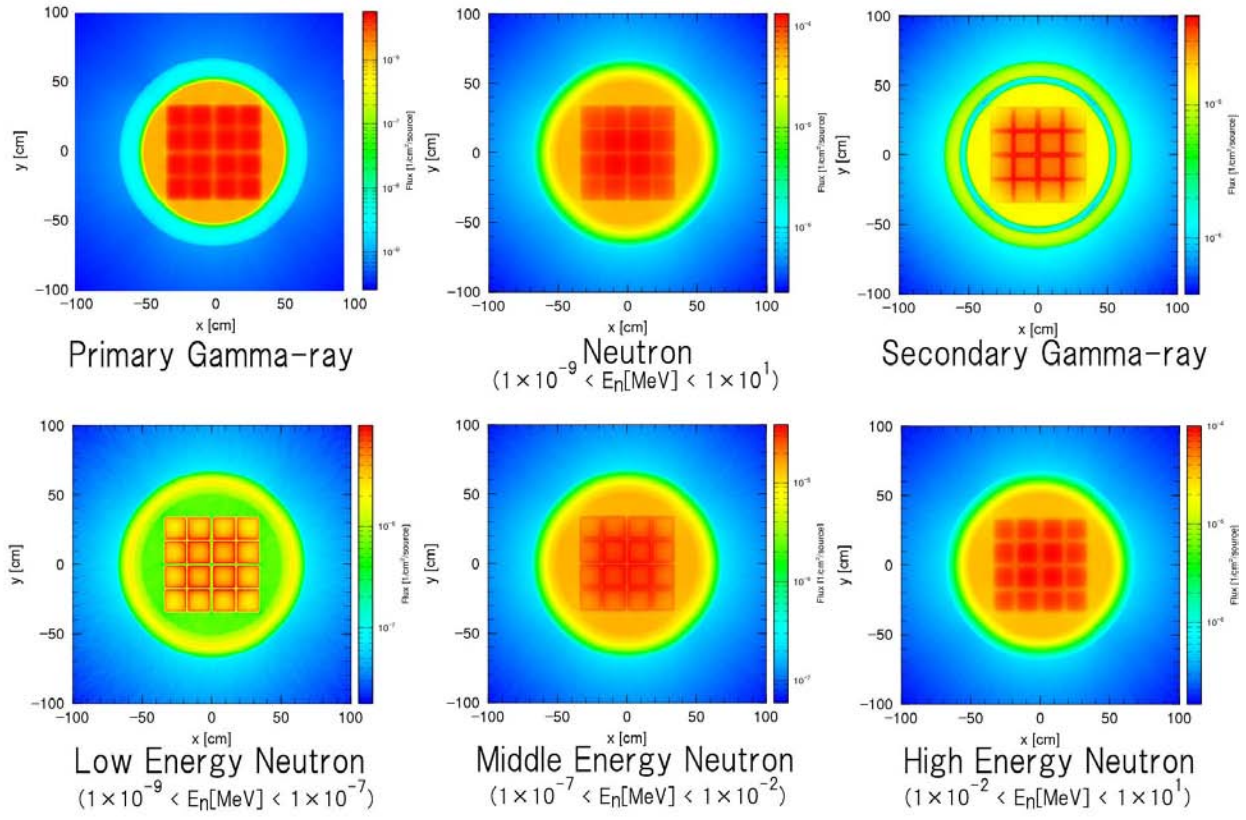

(-7.5 < z[cm] < 7.5)

Fig. 3 Track Length Tally Outputs of Results of Analysis Using Undamaged Cask Model (PHITS Outputs)

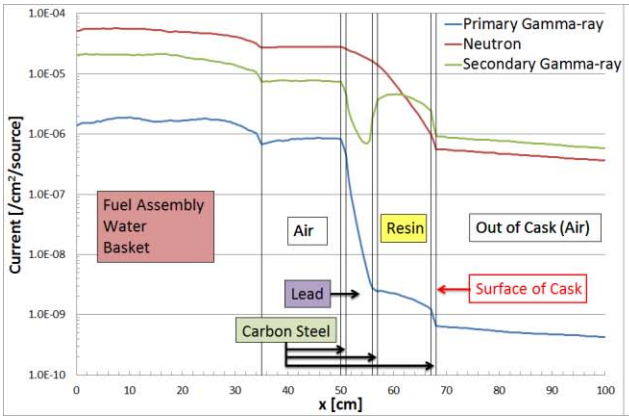

This graph corresponds to the upper three diagrams in Fig. 3.

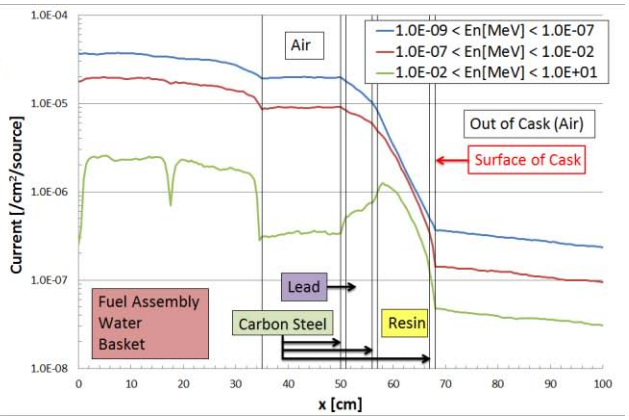

This graph corresponds to the lower three diagrams in Fig. 3.

Fig. 4 Outputs of Results of radiation current Analysis Using Undamaged Cask Model (PHITS output values have been converted in Excel.)

RESULTS OF ANALYSIS USING DAMAGE-SIMULATING CASK MODELS

We performed analysis using damage-simulating cask models. Figure 5 shows the variations in current of radiation that have passed through a circle 5.0 cm in diameter on the x axis.

The graphs of neutrons in the middle of Fig. 5 indicate that variations in neutron current also appear in the undamaged lead region. The current in the inner layer region tends to decrease more significantly, the larger the volume of the damaged region. In the resin region, the current tends to attenuate more gently the larger the volume of the damaged region. These facts show that the neutron reverse flow caused by scattering and reflection in the resin region exerts an influence as far as the inner layer region of the fuel cask.

As the result obtained from the above-mentioned behavior of neutrons, the lower graph of Fig.5 shows un-/small damaged models have the amount of generated secondary gamma-ray larger than large damaged models at the lead and the carbon steel regions inside the damaged region.

Graphs of the primary gamma-ray indicate that the primary gamma-ray current monotonously decreases in all models. The current in the inner layer of the resin region tends to decrease more significantly for models with greater damage. In order to understand the behavior of the primary gamma-ray in the shield in detail, Fig.6 shows time variations of the primary gamma-ray current shown in the upper section of Fig.5. The time origin of Fig. 6 is the moment at which the primary gamma-ray is generated in the source region. Figure 6 shows that after the direct component of the primary gamma-ray has passed through the resin region, the current in this region decreases more slowly in the undamaged cask model than in the circumferential channel defect cask model. Figure 7 shows the results of analysis of the passing angles and the time variations of the primary gamma-ray at an evaluation point of x = 60 cm. The passing angle becomes zero in the normal direction of the x axis. Figure 7

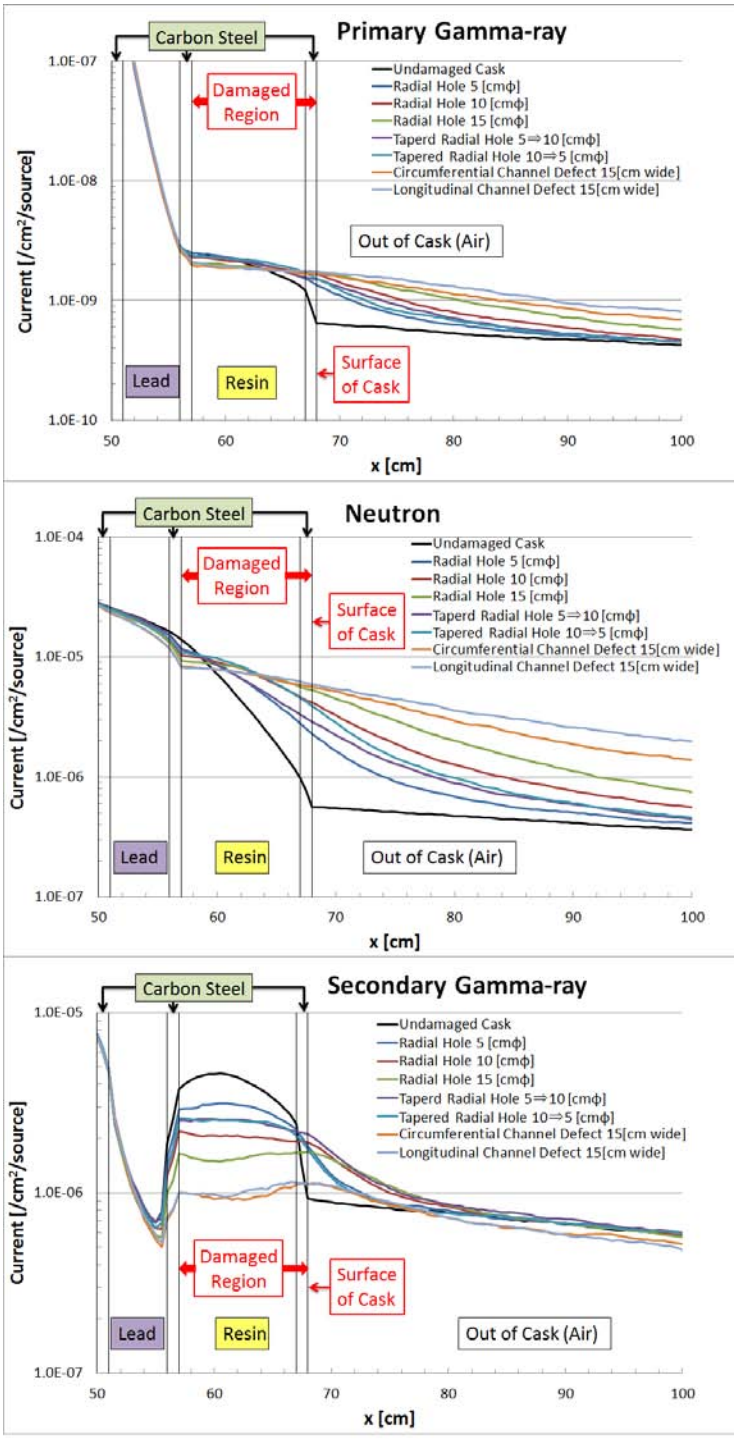

Fig. 5 Variations in Radiation Current in Damage-simulating Cask Models

suggests that compared with damage-simulating cask models, a larger influence is exerted in the undamaged cask model by the back scattered gamma-ray that is incident at a passing angle exceeding 90 degrees from the outer layer. The difference in influence becomes clearer particularly at passing angles close to 180 degrees. From these analysis results, we reached the following conclusion: the influence mainly of the back scattered gamma-ray from the carbon steel region in the outermost layer is weakened in damage-simulating cask models; consequently, the primary gamma-ray current decreases in the inner layer of the resin region.

As previously described, PHITS provides us with functions for outputting various parameters in the form of diagrams, such as two-dimensional distribution charts and graphs. It thereby allows us to clearly express and understand the modes and behavior of radiation propagation in geometries targeted for analysis. Therefore, we expect that PHITS will play an important role in evaluation and understanding the causes and phenomena that occur when unexpected results are obtained when analyzing the dose equivalent rate.

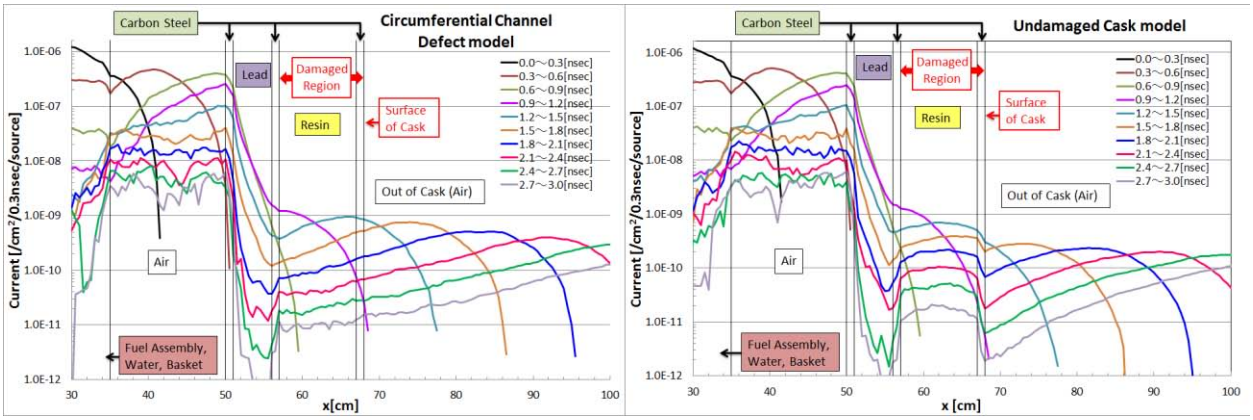

Circumferential Channel Defect model Undamaged Cask model

Fig. 6 Variations in Primary Gamma-ray Current by Transportation Time

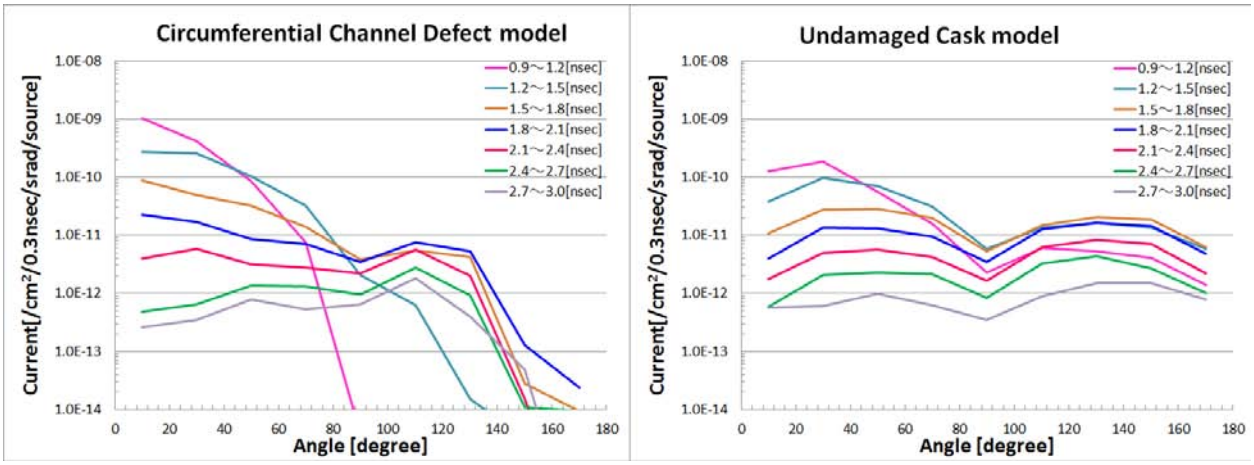

Circumferential Channel Defect model Undamaged Cask model

Fig. 7 Variations in Distribution of Primary Gamma-ray Passing Angle by Transportation Time (x = 60 cm)

EVALUATION OF DOSE EQUIVALENT RATE

Figure 8 shows the relative dose equivalent rates for damage-simulating cask models. These dose equivalent rates have been normalized in the one for the undamaged cask model. The graph on the left-hand side of Fig. 8 shows the relative dose equivalent rates on the surface of the fuel cask. The graph indicates that dose equivalent rates of the primary gamma-ray and neutrons both vary depending on the magnitude of the damage. In addition, the results for the two Tapered Radial Hole models show that the dose equivalent rates of neutrons depend more on the magnitude of the damage to the inner layer than on that of the damage to the outer layer of the resin region. The dose equivalent rates of the secondary gamma-ray decrease more significantly for greater damage to the resin region, the major source of the secondary gamma-ray. However, since the carbon steel in the outermost layer (which has a gamma-ray shielding effect) is also damaged, the dose equivalent rates increase as total compared to those for the undamaged cask model.

The graph on the right-hand side of Fig. 8 shows the relative dose equivalent rates at points 1 m away from the surface of the fuel cask. The dose equivalent rates of the primary gamma-ray and neutrons both correlate with the area of the radiation source region which can be seen from the evaluation point without shielding materials, where the Converted Source Area shown in the graph is the cubic root of the area of the radiation source region mentioned above. For the dose equivalent rates of the secondary gamma-ray, the five Radial Hole models exhibit almost no significant differences. However, the two Channel models with greatly damaged resin regions exhibit a tendency toward slight decreases.

We compared the dose equivalent rate for the Circumferential Channel Defect model (right-hand side of Fig. 2) and that for the 15-cm-diameter Radial Hole model (left-hand side of Fig. 2). The Circumferential Channel Defect model is frequently used for penetration hole simulation in a two-dimensional model expressed in a cylindrical system. The 15-cm-diameter Radial Hole model is used for simulating actual penetration holes more accurately in a reproducible manner in a three-dimensional model. Table 1 shows the comparison results. The values shown in Table 1 vary depending on factors such as the shape of the fuel cask and the thickness of shields; the total dose equivalent rates are determined by the intensity ratio of radiation from each radiation source. The legally specified level is stricter for points 1 m away from the surface of the fuel cask than for the surface. However, the dose equivalent rate for the Circumferential Channel Defect model is expected to significantly exceed that of the 15-cm-diameter Radial Hole model at the evaluation points. Therefore, the penetration hole model in the two-dimensional geometry has a sufficient margin of safety.

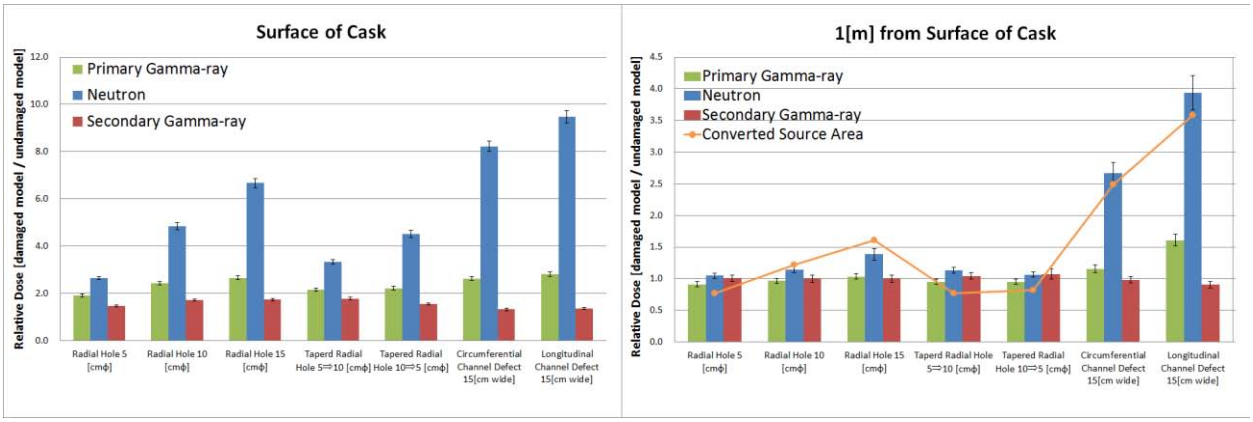

Fig. 8 Relative Dose Equivalent Rate for Damage-simulating Cask Models

Table 1 Dose Equivalent Rate Ratios
(Circumferential Channel Defect model / Radial Hole 15[cmϕ] model)

		Surface of Cask		1[m] from Surface of Cask	
Primary Gamma-ray		0.99 (0.04)		1.12 (0.06)	
Neutron	**Sum**	1.23 (0.04)	1.23 (0.04)	1.93 (0.16)	1.91 (0.16)
Secondary Gamma-ray		0.76 (0.03)		0.98 (0.06)	

(FSD)

CONCLUSIONS

We are aiming to apply the PHITS three-dimensional continuous energy Monte Carlo code to shielding safety analysis of nuclear fuel casks. We used PHITS to analyze the shielding performance of a simulated nuclear fuel cask geometry. The analysis was performed for the undamaged cask model and seven damage-simulating cask models. We examined the analysis results by comparing two-dimensional dose distribution charts, variations in radiation current, and dose equivalent rates. This process allowed us to demonstrate that PHITS can be used to simulate the specific behavior of radiation in the fuel cask. We also compared the dose equivalent rate for the Circumferential Channel Defect model with that for the 15-cm-diameter Radial Hole model. Through this comparison, we were able to evaluate the margin of safety of the two-dimensional penetration hole model for these geometries in this paper. Therefore, we conclude that PHITS provides us with various functions that are effective in performing shielding safety analysis of nuclear fuel casks. We will take further steps, such as establishing optimal analytical methods as well as examining and analyzing such methods, in order to realize practical application of PHITS to shielding safety analysis of nuclear fuel casks.

REFERENCES

(1) K. Niita, et.al., PHITS: Particle and Heavy Ion Transport code System, Version 2.23, JAEA-Data/Code 2010-022(2010)

(2) WA Rhoades, FR Mynatt - CCC-276, 1977

(3) X-5 Monte Carlo Team ”MCNP – A General Monte Carlo N-Particle Transport Code, Version5, Volume I : Overview and Theory,” LA-UR-03-1987, Los Alamos National Laboratory (2003)

(4) K. Niita, et.al., Nucl. Inst. and Meth. **184**, 3 pp.406-420 (2001)

(5) M. Harada, et.al., J. Nucl. Material **343**, 197 (2005)

(6) H. Kumada, et.al., J. Phys. : Conf. Ser. **74**, 021010 (2007)

(7) T. Sato, et.al., Radiat. Res. **171**, 107 (2009)

(8) L. Sihver, et.al., Radiat. Environ. Biophys. 49, 351 (2010)

(9) T. Sato, et.al., Radiat. Environ. Biophys. 50, pp.115-123 (2011)

(10) ICRP Publ.74